Soft Matter

# Physical Aging of Hydroxypropyl Methylcellulose Acetate Succinate *via* Enthalpy Recovery



| | |
|---|---|
| Journal: | *Soft Matter* |
| Manuscript ID | SM-ART-09-2022-001189.R1 |
| Article Type: | Paper |
| Date Submitted by the Author: | 09-Oct-2022 |
| Complete List of Authors: | Seo, Yejoon; Princeton University, Chemical and Biological Engineering<br>Zuo, Biao; Zhejiang Sci-Tech University, Deoartment of Chemistry<br>Cangialosi, Daniele; CSIC, Centro de Fisica de Materiales<br>Priestley, Rodney; Princeton University, Chemical and Biological Engineering |
| | |

# Physical Aging of Hydroxypropyl Methylcellulose Acetate Succinate *via* Enthalpy Recovery

*Yejoon Seo[1], Biao Zuo[2], Daniele Cangialosi[3,4], Rodney D. Priestley[1,5*]*

[1]Department of Chemical and Biological Engineering, Princeton University, Princeton, New Jersey 08540, United States of America

[2]Department of Chemistry, Zhejiang Sci-Tech University, Hangzhou, 310018, China

[3]Donostia International Physics Center (DIPC), Paseo Manuel de Lardizábal 4, 20018, San Sebastián, Spain

[4]Centro de Fisica de Materiales (CSIC-UPV/EHU), Paseo Manuel de Lardizábal 5, 20018, San Sebastián, Spain

[5]Princeton Institute for the Science and Technology of Materials, Princeton University, Princeton, New Jersey 08540, United States of America

* Corresponding Author: Rodney D. Priestley

Full Address: 41 Olden St, A215 Chemical and Biological Engineering, Princeton, New Jersey, 08540

E-mail Address: rpriestl@princeton.edu

Telephone: 609-258-5721

Fax: 609-258-5599

**Abstract**

Amorphous solid dispersions (ASDs) utilize the kinetic stability of the amorphous state to stabilize drug molecules within a glassy polymer matrix. Therefore, understanding the glassy-state stability of the polymer excipient is critical to ASD design and performance. Here, we investigated the physical aging of hydroxypropyl methylcellulose acetate succinate (HPMCAS), a commonly used polymer in ASD formulations. We found that HPMCAS exhibited conventional physical aging behavior when annealed near the glass transition temperature ($T_g$). In this scenario, structural recovery was facilitated by α-relaxation dynamics. However, when annealed well below $T_g$, a sub-α-relaxation process facilitated low-temperature physical aging in HPMCAS. Nevertheless, the physical aging rate exhibited no significant change up to 40K below $T_g$**,** below which it exhibited a near monotonic decrease with decreasing temperature. Finally, infrared spectroscopy was employed to assess any effect of physical aging on the chemical structure of HPMCAS, which is known to be susceptible to degradation at temperatures 30K above its $T_g$. Our results provide critical insights necessary to understand better the link between the stability of ASDs and physical aging of the glassy polymer matrix.

## Introduction

The low aqueous solubility for the high number of newly-discovered drug molecules remains a pervasive challenge in the field of controlled drug delivery.[1,2] In the case of oral drug delivery, the drug concentration gradient across the membrane of the gastrointestinal tract directly influences the bioavailability of the drug substance.[1] Poor aqueous solubility reduces this concentration gradient, resulting in low bioavailability. This state of affairs presents the enduring challenge of achieving the high dose requirement for drugs with low bioavailability without exacerbating relevant negative consequences (e.g., high material demand and associated waste, drug product instability, pill burden and its detrimental effect on patient compliance,[3,4] etc.). Addressing this challenge makes the design and formulation of oral drug products difficult and complex. However, many formulation strategies have been developed through the clever application of pre-existing technologies.[5–12] These strategies are currently commercially utilized to circumvent the poor solubility issue and increase oral bioavailability.

One of the most promising approaches for increasing the bioavailability of low solubility drugs is amorphous solid dispersions (ASDs).[13–15] ASDs are composed of an active pharmaceutical ingredient (or drug) that is molecularly dispersed into a glassy polymer matrix, creating a solid dispersion in the amorphous state. The technique skillfully exploits the glassy polymer excipient's disordered structure and reduced mobility to stabilize the drug in an amorphous state. Upon dissolution of the ASD, the amorphous drug molecules are stabilized by the polymer excipient, maintaining their glassy state in solution despite their propensity to recrystallize.[16,17] These stabilized drug-polymer particles exhibit a higher apparent aqueous solubility than the pure amorphous drug and the bulk crystalline form, allowing for much higher uptake through the gastrointestinal tract.[18,19] This benefit demonstrates the need to understand the critical aspects of the amorphous state in relation to ASD design and performance.

The amorphous state is a non-equilibrium state achieved by rapid cooling of a glass-forming liquid from the equilibrium melt state to the glassy state.[20] At the glass transition, there is no change in the material structure.[21] Despite this fact, the glassy state exhibits structural rigidity and a modulus on the order of $10^9$ Pa. Glasses are

thermodynamically out of equilibrium and possess excess energy with respect to the equilibrium state. Therefore, when a glassy material is held isothermally below the glass transition temperature ($T_g$), its thermodynamic properties (e.g., volume and enthalpy) evolve towards the equilibrium to a more stable state, through a spontaneous process called glassy-state structural relaxation.[22,23] Accompanying structural relaxation are changes in the physical properties of the glassy material that significantly affect its performance and function – a process termed physical aging. To quantify the extent of structural relaxation or physical aging in the amorphous state, Tool defined the fictive temperature ($T_f$).[24] The concept of the fictive temperature and its calculation *via* calorimetric measurements have been employed generally across different polymers and model systems.[25–29] In all cases, the calculation is vital to determining the evolution of physical properties over time in the glassy state. Additionally, $T_f$ measurements at longer aging times ($t_a$s) capture the behavior of aged glasses as they approach the equilibrium state. Interpolating such data yields essential parameters such as the aging rate and the time required to reach equilibrium. Undoubtedly, structural relaxation will influence the performance of ASDs, which rely on the stability of the glassy state to stabilize drug molecules against crystallization.[30]

Recent studies of the physical aging behavior of various materials suggest the possible existence of intermediate equilibrium glassy states, challenging the conventional understanding whereby one explicit equilibrium is approached over time.[31–40] This proposition is evidenced by sub-$T_g$ endotherms that are decoupled from the glass transition, particularly in polymer systems annealed at temperatures well-below the system $T_g$. Hodge *et al*. first observed and modelled these sub-$T_g$ endotherms in polymer systems,[41,42] but the exact physical origins remain unclear.[43] In the case of ASDs, the implications of these endotherms are particularly meaningful, as ASDs are typically stored and processed at temperatures well-below $T_g$. For example, intermediate equilibrium glassy states would obfuscate the glassy behavior of the system, making it more challenging to predict ASD stability during storage and use. This unique consideration presents a new design constraint for ASDs, the ramifications of which we know very little. Together with the importance of the amorphous state for ASD stability, these recent findings pose a unique opportunity to further our knowledge of the intricate relationship

between the amorphous state and ASD performance. Of particular interest is the possibility that physical aging deep in the glassy state, at temperatures relevant to storage of ASDs, might promote a different mode of relaxation towards equilibrium.[35,44]

However, investigating this relationship directly *via* calorimetric studies is challenging, particularly because ASDs are multi-component systems. They primarily consist of a drug and polymer, but may require additional excipients as needed. Even when disregarding these additional excipients and focusing on the binary drug-polymer system, phase separation may occur, driven by the system's affinity for thermodynamic stability.[45] In turn, phase separation is further influenced by relative drug-polymer concentrations, drug-polymer interactions, and environmental factors (e.g., high relative humidity and storage temperature).[46,47] Upon phase separation, the drug molecules no longer remain stable in the polymer matrix and may begin to crystallize, compromising the benefit of ASD technology.[48–55] Naturally, the effect of physical aging on phase separation and, consequently, drug stability in the dispersion comes into question. On the one hand, the densification of the glassy polymer that follows upon aging is expected to kinetically stabilize drug molecules within the glass, preventing drug recrystallization in the matrix. At the same time, the thermodynamic drive towards glassy equilibrium tends to draw drug molecules together, promoting drug recrystallization as physical aging concentrates the drug molecules *via* densification. Therein lies the paradoxical and complex nature of the interplay between physical aging and ASD drug stability. This relationship has been most often explored using equilibrium measurements on as-processed polymers and ASD systems subjected to isothermal annealing protocols (i.e., stability studies), high relative humidity, or added water content.[56–61] However, there remains a dearth of studies on the non-equilibrium physical aging behavior of pharmaceutical polymer systems,[62–64] with only one recent study by Lapuk *et al*. on poly(vinylpyrrolidone).[65] This dearth represents the challenge of accurately investigating the implications of drug presence on the physical aging of the multi-component ASD system, prompting a study on a pure polymer excipient system. Therefore, this current work seeks to contribute complementary isothermal calorimetric physical aging studies, in which aging proceeds from equilibrium, on another common polymer excipient used in the pharmaceutical industry.

For this study, we selected hydroxypropyl methylcellulose acetate succinate (HPMCAS) as the model polymer excipient. HPMCAS is a highly functionalized natural cellulose derivative and is provided in three grades with ranging acetyl and succinyl side group content.[66,67] These three grades offer a range of hydrophobicity and pH activity as needed for their application.[67] A specific grade of HPMCAS may be selected to best promote drug-polymer interactions or to dissolve and release the drug at a specific point in the digestive tract. Despite such multi-purpose utility for pharmaceutical systems, the physical aging behavior of pure HPMCAS has yet to be fully explored. Here, we performed physical aging studies on HPMCAS at aging temperatures ($T_a$s) of 313K, 333K, 343K, 353K, 363K, 373K, 383K, 388K for aging times up to 600 min. We demonstrate the distinct mechanisms for physical aging of HPMCAS at $T_a$ near $T_g$ and below $T_g$ – 40K. The aging behavior well below $T_g$ breaks from convention as there is significant thermodynamic evolution at temperatures as low as $T_g$ – 80K, where kinetic stability is expected to be dominant.[68] The low-temperature relaxation is not due to the normal α-relaxation dynamics but an entirely different mode of relaxation more pertinent to local secondary relaxation or sub-α-relaxation. These results call into question the mechanisms through which the low-temperature relaxation occurs and in turn, the perceived drug stability in HPMCAS formulations.

## Experimental Methods

**Materials.** The HPMCAS (see chemical structure in **Figure 1**) was provided by Lonza Pharma. Specifically, three grades of AQOAT® from Shin-Etsu Chemical Co. were provided: HPMCAS-LF, -MF, and -HF. Each grade of HPMCAS has a different percentage of the total mass consisting of acetyl and succinyl groups: LF with acetyl and succinyl mass percentages of 8% and 15%, MF with 9% and 11%, and HF 12% and 7%, respectively. Polystyrene (PS) was used as a model system to compare its physical aging behavior to HPMCAS. The PS (weight-average molecular weight 16,400 g/mol) was purchased from Polymer Source Inc. and used as received. Succinic acid was purchased from Sigma® and used as received.

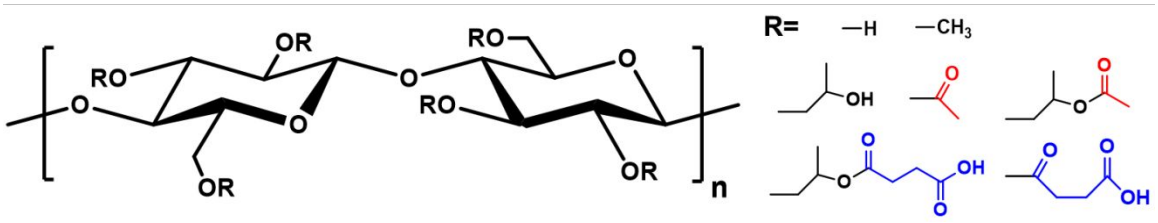


**Figure 1.** Chemical structure of HPMCAS. The acetyl and succinyl groups are highlighted in red and blue, respectively.

**Thermal Analysis Equipment.** A Thermogravimetric Analyzer Q50 (TA Instruments) was used to establish the temperature range of analysis for HPMCAS. A 5 – 10 mg sample of HPMCAS was placed in a platinum pan and heated to 873K at 20K/min under an inert nitrogen atmosphere, during which the mass of the sample was measured.

Differential scanning calorimetry was used to measure glass transitions and physical aging. All calorimetric measurements and physical aging experiments were performed using a differential scanning calorimeter (DSC) 2500 (TA Instruments) equipped with an RCS90 cooler. The DSC furnace chamber was constantly flushed with nitrogen. Approximately 5 mg of material were placed into aluminum hermetically-sealed pans with a pinhole on the sealed lid so that any residual moisture or volatiles may escape during thermal analysis. A pinhole was also made in the reference pan for parity between sample and reference. Temperature calibrations were performed for the DSC using a melting temperature measurement for indium, and heat capacity calibrations were performed using sapphire standards.

**Methodology of $T_g$ and $T_f$ Calculation.** All reported $T_g$ were calculated on heating using available tools in the TRIOS software. The $T_g$ calculation tool computed the midpoint $T_g$. The $T_g$ of the primary polymer studied in this work, HPMCAS-LF, was calculated to be 392.8 ± 0.2K. A table containing the $T_g$ values of all polymers in the study is presented in the supporting information (**S.I. Table 1**).

For a given down-jump aging experiment to the annealing temperature, $T_a$, samples were annealed between 1 – 600 min. The evolution of aging was monitored by determining $T_f$ as a function of time. All of the re-heating step data, including the unaged reference curve were compiled and processed to calculate $T_f$ using a custom Python script created by Abate *et al*.[69] After minimizing the mean squared error between the

unaged reference curve and aging curves outside the temperature range of the glass transition and enthalpy recovery, the Python script employed the Moynihan method of $T_f$ calculation for each aging data.[70] A sample calculation is presented in the supporting information (**S.I. Figure 1**). These $T_f$s were then plotted as a function of $\log_{10}$ time. A slope representing the aging rate at a given $T_a$ was obtained by applying a linear fit of the $T_f$ data for the range of time that yields the greatest R-square value.

**TGA Analysis.** The TGA data for HPMCAS-LF is shown in **S.I. Figure 2**. The onset of degradation started at ~ 473K. To confirm chemical and thermal stability at and below this temperature, we performed isothermal degradation studies at the following temperatures: 398K, 403K, 413K, 423K, 443K, 473K. These results revealed a negligible mass loss rate (<0.01 mg per hour) at temperatures below 423K. Considering the TGA results and thermal stability data provided by the manufacturer, we determined 423K to be the maximum temperature for calorimetric studies. This maximum temperature allowed for a well-defined melt line for all aged heat capacity data, which is crucial for $T_f$ determination. We also note that overlapping melt lines served as another indication of negligible degradation. The TGA data for HPMCAS-MF and -HF are presented in supporting information (**S.I. Figures 3 and 4)**, and both exhibit similar degradation behavior to HPMCAS-LF.

**Aging Protocol.** The thermal protocol for physical aging is schematized in **Figure 2**. All cooling and heating steps were performed at 20K/min. Prior to aging, the polymers were heated to 403K and held isothermally for 10 min to equilibrate and erase thermal history. In addition, the isothermal step ensured the removal of any moisture. For the physical aging component, the samples were cooled to the desired $T_a$ and held isothermally at aging times from 1 up to 600 min. After aging, the samples were cooled to a low temperature and re-heated to 423K; this heating step recorded the sample response and featured the typical endothermic peak indicative of enthalpy recovery. Upon re-heating to 423K, the samples were held isothermally to erase thermal history before undergoing the next aging cycle. After the final re-heat for the 600 min aging, the samples were again cooled and re-heated twice to obtain the post-aging reference curve. When compared to the unaged reference curve, this post-aging curve acts as a check to ensure the

amorphous properties of the samples were not affected during the aging protocol. Generally, such checks are performed after each aging step instead of only at the end of a series of aging steps. Experiments where the checks after each aging step were included showed that the isothermal hold after each aging step was sufficient to erase any aging effect. Ultimately, these checks between aging steps were removed to reduce any potential thermal degradation effects by reducing the total experimental time at temperatures above $T_g$. Though the TGA results indicated a negligible level of degradation at the maximum temperature, degradation would no longer be negligible at sufficiently long protocol times.

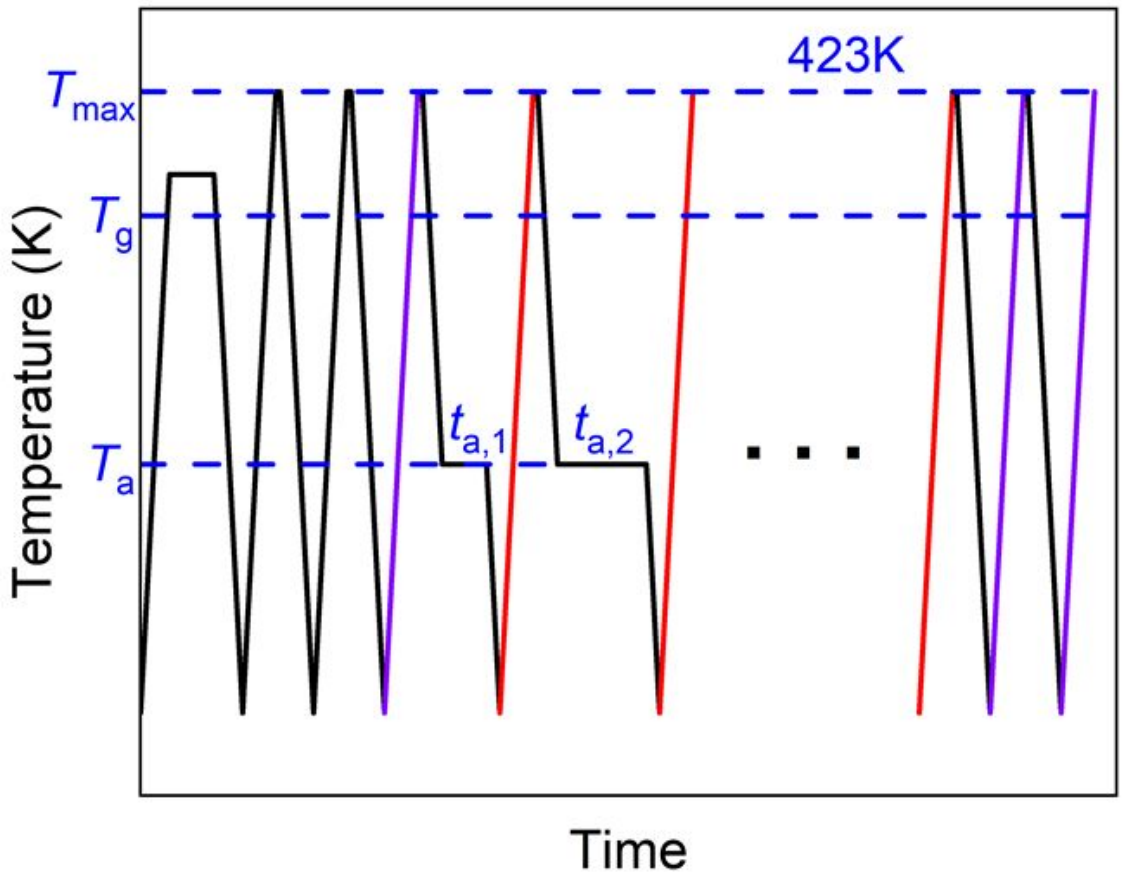


**Figure 2.** Illustration of the physical aging protocol employed in this study. The sample was aged at $T_a$ for $t_a$ (solid blue lines) up to 600 min and the subsequent thermogram on re-heating (red lines) was collected and analyzed for $T_f$ calculation. At the end of the protocol, the reference curve was reproduced and compared with the first reference curve (purple lines) to ensure that there was no significant degradation.

**FTIR Measurements.** A Nicolet iN10 MX (Thermo Scientific, Waltham, MA) was employed for FTIR measurements on unaged and aged HPMCAS-LF and succinic acid. Aged HPMCAS-LF were prepared using a protocol similar to that of physical aging. The samples were heated to 403K and held isothermally for 10 min. Upon re-heating to 423K, the samples were cooled to either 353K or 388K and aged up to 600 min. These samples were then cooled to room temperature and immediately taken for FTIR analysis. The detectors were cooled using liquid nitrogen before data collection. Two hundred fifty-six measurement scans at different locations for all of the samples were taken and compiled to generate the absorbance plots with the Kubelka-Munk function applied.

## Results and Discussion

**Physical Aging Behavior.** The calorimetric data obtained on heating after aging HPMCAS-LF for up to 600 min were compiled in **Figure 3**. At $T_a$ above 373K (**Figure 3a, b, c**), pronounced endothermic peaks appeared near $T_g$. These endothermic peaks were representative of enthalpy recovery that occurred at $T_g$ and grew with increasing $t_a$. In agreement with classic observations of physical aging, this trend represented the access to the α-relaxation process for enthalpy recovery, where the growing endothermic peak reflected the similarly increasing extent of structural relaxation over $t_a$.

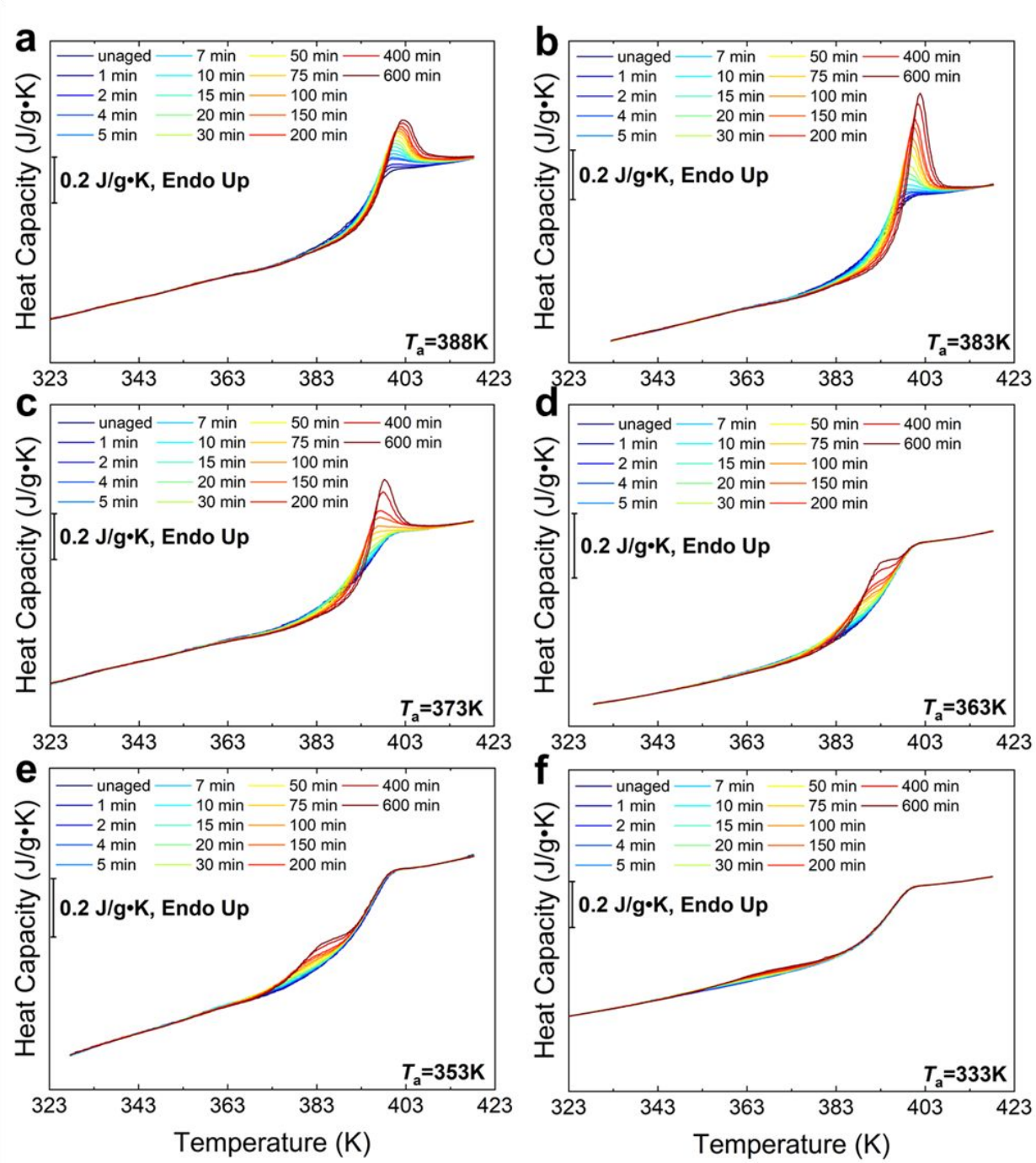


**Figure 3.** A compilation of re-heating thermograms after aging at $t_a$ for $T_a$ = **(a)** 388K, **(b)** 383K, **(c)** 373K, **(d)** 363K, **(e)** 353K, **(f)** 333K.

At $T_a$ = 363K (**Figure 3d**), the endothermic peaks began to decouple from the specific heat step underlying the glass transition. The extent of this decoupling was dependent on $t_a$. With short $t_a$, the decoupling was complete as the broad endotherm was

resolved before the $T_g$. In contrast, at long $t_a$ the endothermic peak was sharper and resolved near $T_g$.

The complete decoupling of enthalpy recovery and the glass transition at all $t_a$ examined was evident for samples aged at $T_a$ well below $T_g$ ($T_a < T_g - 40K$) (**Figure 3e, f**). This is in direct contrast to the observed behavior at $T_a$ near $T_g$ (**Figure 3a, b, and c**), where the endotherms were primarily resolved near $T_g$. The complete decoupling at $T_a$ below $T_g$ – 40K hinted at the presence of a different enthalpy recovery mechanism that does not involve α-relaxation. This additional mechanism was accessed at low $T_a$ but was able to fully recover the effects of physical aging such that the α-relaxation was accessed only to devitrify the polymer.

Such behavior does not agree with the current conventional understanding of physical aging. Previous attempts by Hodge *et al*. to describe this low temperature endotherm exclusively on the basis of the α-relaxation via the Tool-Narayanaswamy-Moynihan model[71] required atypical small stretching exponents and/or non-linear parameters (<0.3).[41,42,72] While HPMCAS exhibits chemical complexity during physical aging, as discussed below, it is worth noting that similar low temperature peaks have been observed in other glasses aged well below $T_g$ including metals,[31,73,74] polymer nanospheres,[32,33] polyethers,[35] a plastic crystal,[75] phase change materials,[76] sucrose,[77] and other polymers with vastly different structures.[36,44,78–80] In this regard, our work contributes to the general discussion on the lower temperature aging response of glasses. Regardless of the origin of this phenomenon, its implications can have a significant impact on the view of drug stability in HPMCAS ASDs, i.e., the focus of the current study.

Auxiliary aging studies were performed to vet these findings further and provide a comparative measure for the observed physical aging behavior. First, to determine if the composition of the side groups had any effect on the lower temperature aging behavior, the other two grades of HPMCAS (HPMCAS-MF and -HF) were aged at $T_a$ = 388K and 353K (**S.I. Figures 5 and 6**). Both grades exhibited the same low temperature aging behavior as HPMCAS-LF, where enthalpy recovery on heating was completed before $T_g$. Second, to exclude the possibility that the observations were due to an artifact of the instrument or data analysis procedure, 5 – 10 mg of PS was aged at four different

temperatures, with the lowest temperature being $T_g$ – 50K (**S.I. Figure 7**). All PS samples were subjected to a similar aging protocol described previously, with the only change being the total temperature range. PS did not exhibit the same broad endothermic peaks as HPMCAS, even at $T_a = T_g$ – 50K (relative $T_a$ where HPMCAS showed noticeable low-temperature endotherms on heating). Instead, PS showed minimal enthalpy recovery near $T_g$ (**S.I. Figure 7d**). These additional studies provide evidence, to an extent, that the observed physical aging behavior was a material property of HPMCAS, but not unique to it.

In the context of HPMCAS as a polymer excipient in ASDs, this behavior is of interest as these low $T_a$s begin to resemble ambient temperatures used for stability studies required for drug product approval. Despite the seemingly low extent of enthalpic recovery at these $T_a$s (**Figure 3e**, **f**), the endotherms reflecting this process remained noticeable even at the time scale of 600 min, a relatively short $t_a$ with respect to those employed in stability studies that reach at least several months in scale.

**Aging Rate Analysis. Figure 4** compiles and illustrates the change in $T_f - T_a$ over the $\log_{10} t_a$ at each $T_a$. The $T_a$ was subtracted from the $T_f$ as $T_a$ represents the theoretical limit of $T_f$ at infinite $t_a$. As expected, each set of $T_f$s exhibited a decreasing trend over time. At $T_a$ near $T_g$, signs of plateau approach were visible at longer aging times. One notable observation in **Figure 4** was that despite signs of $T_f - T_a$ plateau, the $T_f - T_a$ values did not explicitly reach 0 for $T_a$ near $T_g$ after 600 min of aging. This behavior indicated a partial enthalpy recovery at long $t_a$ even when aged at temperatures near $T_g$, in line with behaviors observed with other polymer systems.[81]

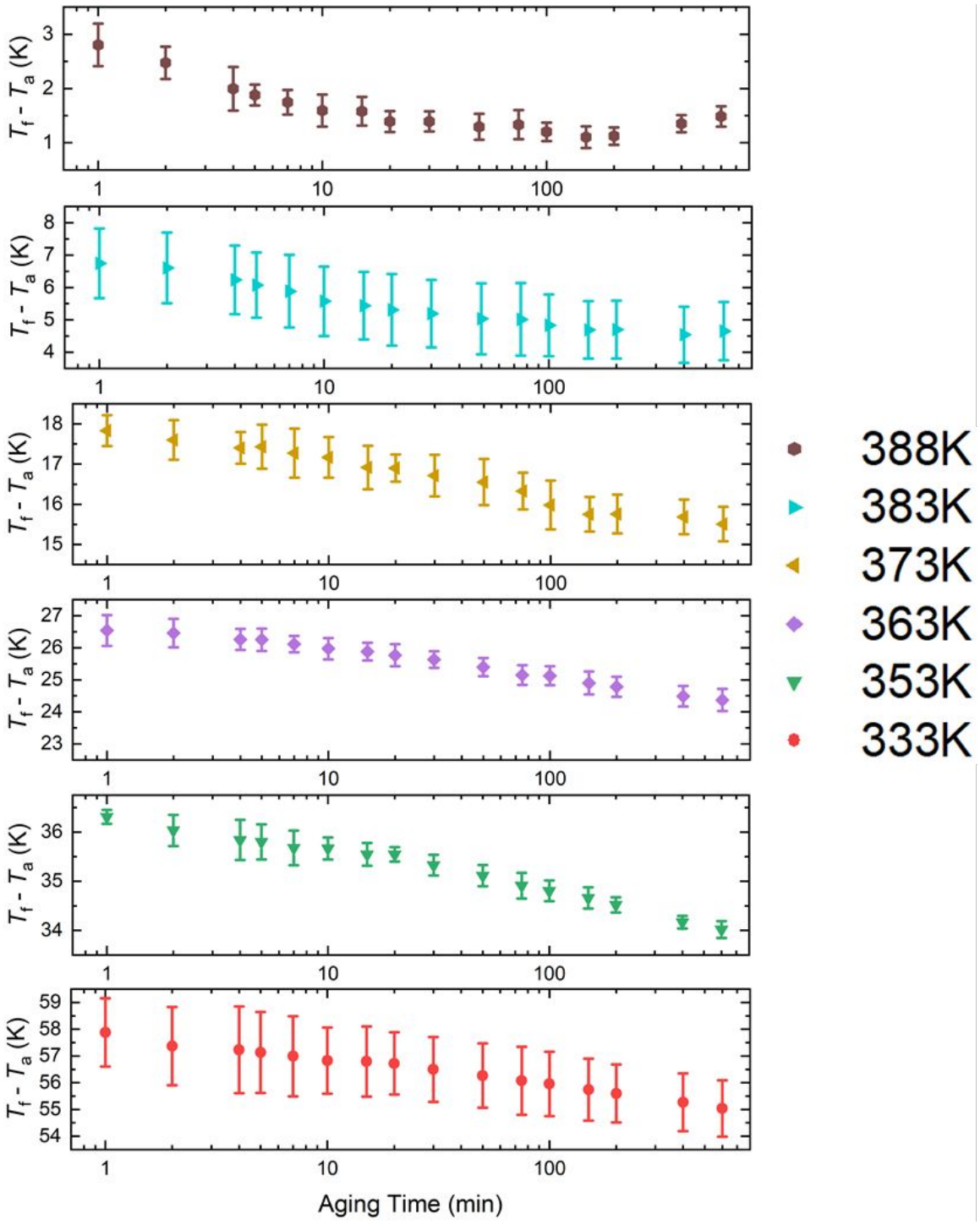


**Figure 4.** The evolution of $T_f - T_a$ over time for each $T_a$. We note the $T_f$ plateau for $T_a$ = 388K, 383K, and 373K within 600 min of aging.

A linear fit of the $T_f - T_a$ data in **Figure 4** produced the aging rate at a given $T_a$, represented by the slope of the linear fit. Additional information (e.g., fit range, aging rate, R-square value) on the linear fits for each of the $T_a$s is available in the supporting

information (**S.I. Table 2**). **Figure 5** presents the aging rate of HPMCAS-LF as a function of $T_a$. A general decreasing trend was apparent over the range of $T_a$s investigated. More importantly, there were two regimes over the $T_a$ range with different behaviors. At $T_a$ near $T_g$, the aging rate remained relatively stable as $T_a$ decreased. Once $T_a$ decreased to below 353K ($T_g$ – 40K), the aging rate decreased significantly. This trend in the aging rate was similar to that seen in other bulk polymer systems, where with decreasing $T_a$, the aging rate increased to a maximum and then decreased.[82–85] Though the aging rate of HPMCAS-LF near $T_g$ was stable before it decreased, the general trend was reflected. More notably, the transitional regime between these two behaviors ($T_a$ = ~343K – 363K) coincided with the temperature range in which the continuous shift of endotherms toward lower temperatures led to full enthalpy recovery below $T_g$, as seen in the change across **Figure 3d-f**. These different regimes suggested that there exists a secondary mechanism that affected the polymer aging rate. According to conventional temperature dependence of the α-relaxation time, if the α-relaxation was solely responsible for HPMCAS aging at low $T_a$, the aging rate should approach zero at the $t_a$ examined in this study. The contrary evidence in **Figure 5** indicated significant thermodynamic evolution in HPMCAS at low $T_a$, likely through a secondary relaxation mechanism. However, evidence of the low $T_a$ kinetic stability remained as signified by the notable decrease in the aging rate.

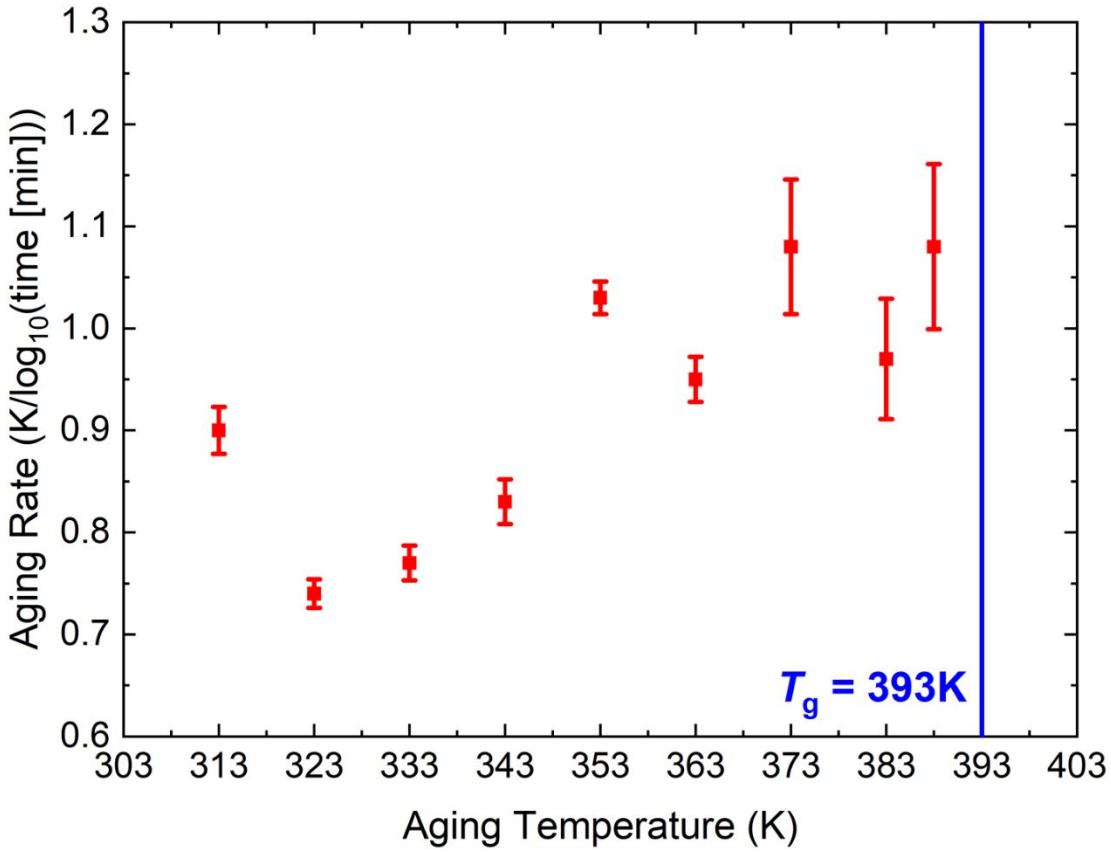


**Figure 5.** The aging rate of HPMCAS as a function of $T_a$.

The origin of the low-temperature aging behavior remains a heavily discussed topic in the field, with several possible explanations: Johari-Goldstein β-relaxations having similar properties to that of the α-relaxation,[86] sub-Rouse modes[87] resulting from the intrinsic heterogeneous nature of glass relaxation,[88] a recently identified slow Arrhenius mode,[89] an alternative equilibrium mechanism separate from the absolute glassy equilibrium state,[32,35,44] or other sources related to the experimental process itself.[90] Though the exact origin remains debated, HPMCAS undoubtedly exhibited similar physical aging behavior to several different systems, where a low-temperature endotherm is present and completely decoupled from the glass transition event.[35,39,91] Regardless, there exist differences specific to this polymer system that require separate and further consideration.

TGA data confirmed that HPMCAS does not degrade below 473K under an inert atmosphere when heated at standard rates. Nevertheless, due to the large time scales

involved, HPMCAS-LF undergoes modifications to its chemical structure over time during physical aging. **Figure 6a** shows FTIR spectra of HPMCAS-LF as it was aged at 388K, represented by FTIR spectra taken immediately after aging. A similar data set for HPMCAS-LF aged at 353K is available in supporting information (**S.I. Figure 8**). There were no notable differences in the observed chemical changes between HPMCAS-LF aged at 388K and 353K. The highlighted region **1** in **Figure 6a** shows the broadening of IR peaks representative of changes to the chemical environment of the hydroxyl (-OH) groups. This peak broadening reflected the internal manufacturer-provided thermal stability data, where heat treatment at 423K resulted in free succinic acid content. The free succinic acid produced a new range of chemical environments for -OH groups (proposed mechanism illustrated in **Figure 6b**), resulting in the broadening of the peaks in that region. This particular chemical change was not expected to have impacted the glassy state of the polymer system since the reference curves obtained before and after the aging protocol remained identical across all $T_a$.

Furthermore, the highlighted region **2** in **Figure 6** shows the development of two distinct features over the course of physical aging. A small broad peak developed near 2100 $cm^{-1}$ and a shouldering of the 1750 $cm^{-1}$ peak occurred. The exact origin of the former remains unclear. However, FTIR analysis of acetylated and succinylated cellulose exhibited this 2100 $cm^{-1}$ peak, though there was no further explicit consideration due to its relatively small magnitude.[92,93] These observations led us to conclude that this feature was not anomalous and did not represent any significant chemical change that affected the polymer system. On the other hand, the developing shoulder feature near 1750 $cm^{-1}$ was commonly present in acetylated cellulose systems as a double peak near the carbonyl range, specifically at 1750 and 1650 $cm^{-1}$.[94–97] Since the untreated HPMCAS did not exhibit the characteristic double peak, we concluded that throughout physical aging, there was an increase in relative representation of acetylated side groups. This conclusion was in line with the thermal stability behavior of HPMCAS that produced the broadening of peaks in the highlighted region **1** in **Figure 6**.

To further vet this hypothesis that free succinic acid content was producing these changes, the FTIR data of the pure succinic acid, aged HPMCAS-LF, and untreated

HPMCAS-LF was compared (**S.I. Figure 9**). The aged HPMCAS-LF and succinic acid spectra shared the broad feature in region **1** and the shouldering peak in region **2**, providing a rudimentary but compelling evidence that confirmed the influence of succinic acid to the chemical environment.

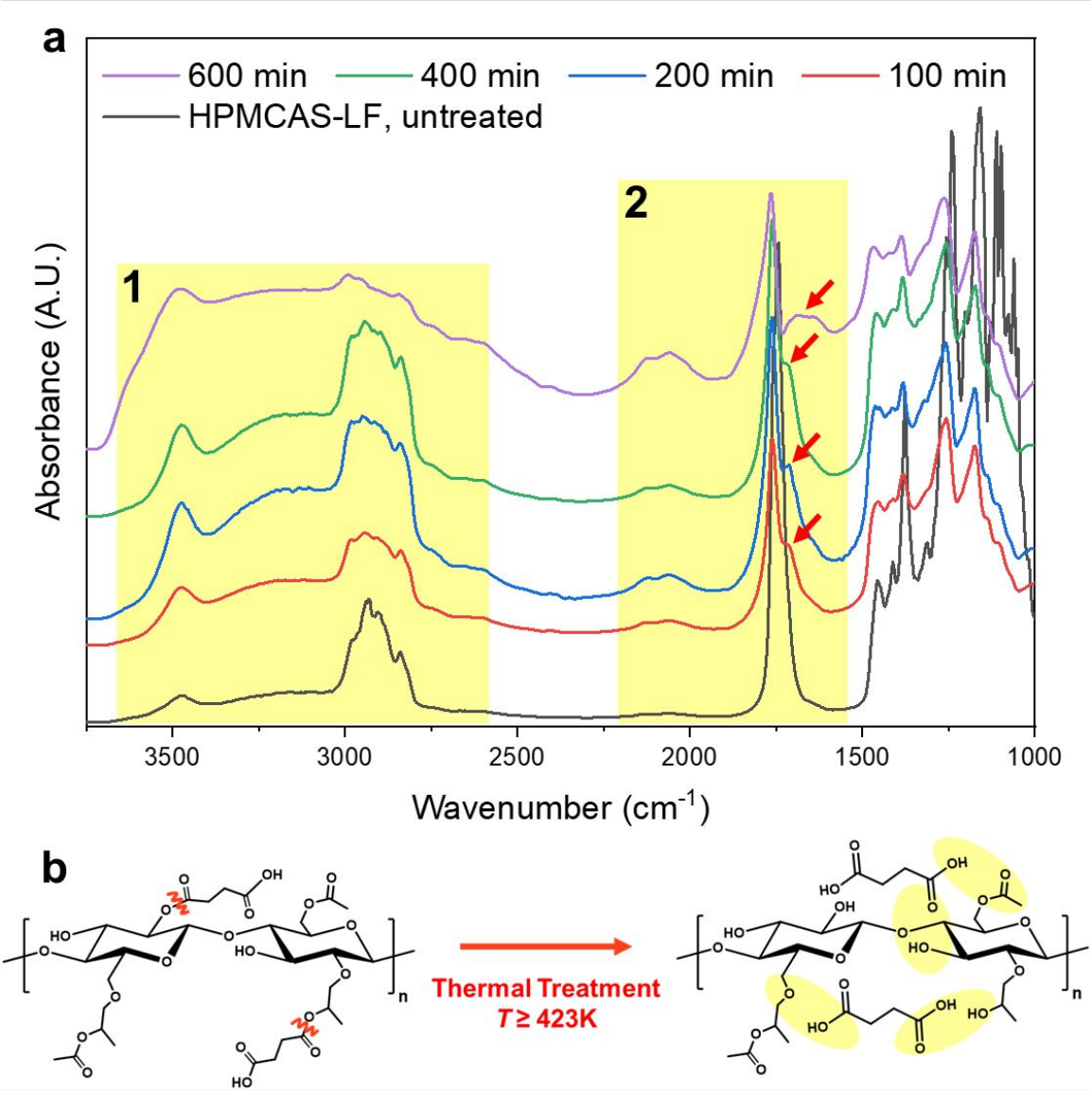


**Figure 6. (a)** FTIR spectra of untreated HPMCAS-LF and HPMCAS-LF aged at $T_a$ = 388K for 100, 200, 400, and 600 min. Features in region **1** broaden with $t_a$, indicating changes to the chemical environment of -OH groups. In region **2**, two features develop with $t_a$: a small broad peak near 2100 $cm^{-1}$ and a shoulder peak that breaks away from the primary 1750 $cm^{-1}$ peak, as denoted by the red arrows. **(b)** The degradation of succinyl groups in HPMCAS producing free succinic acid at temperatures greater than or equal to 423K. The resulting free succinic acid

introduced new chemical environments for various -OH, -CH, and C=O bonds (highlighted in yellow ovals) that contributed to the highlighted changes in **(a)**.

The FTIR spectra confirmed that chemical changes were occurring throughout $t_a$. Additionally, these chemical changes when aged at 388K and 353K were identical. Despite these chemical changes, a comparison of reference curves before and after the aging protocol across all $T_a$s showed no signs of change to $T_g$ or mass loss (i.e., the step change in glass transition remained the same). Considering these observations, we suggest that the low-temperature aging behavior of HPMCAS may only be partially attributed to the free succinic acid content in the sample. The free succinic acid molecules could act as local plasticizers on the scale of the side-groups without affecting the global $T_g$ of the sample. These plasticizing molecules provided the local molecular mobility required to allow the system to partially relieve the physical aging effects at temperatures below the global $T_g$. This rationale applies only to this cellulose derivative and requires further experimental confirmation. Therefore, we acknowledge and reference the ongoing discussions on the potential origins of the observed low-temperature physical aging behavior and that such explanation is not necessary for other systems.[35,39,44,80,86,90]

HPMCAS has long been considered an excellent polymer excipient for ASDs due to its amphiphilic side groups and natural biodegradability.[66] The results in this study offered added insight into how HPMCAS stabilizes drugs in ASDs from the perspective of physical aging. The potential for local molecular mobility below $T_g$ undermines the notion that ASD storage below $T_g$ – 50K guarantees the prevention of drug recrystallization *via* kinetic stability.[68] This property of HPMCAS allowed for enthalpy recovery without tapping into the more global α-relaxation. More importantly, it opened the possibility of notable structural relaxation well-below $T_g$ and implied the access to a thermodynamic pathway to phase separation within ASDs even at $T_a$ as low as 60K below $T_g$. Additionally, the aging rate was comparably lower at $T_a$ < 353K than at $T_a$ > 353K but still well within a magnitude of order across the entire $T_a$ range. This was a quantitative confirmation that even at $T_a$ = $T_g$ – 80K, the HPMCAS-LF system still aged at an appreciable rate. These aging behaviors are of particular interest because thermal processing of polymer excipients and stability testing of ASDs typically require the $T_a$s studied in this work. In such cases, both the physical aging behavior of HPMCAS and the

corresponding chemical changes will play a pivotal role for drug stability in HPMCAS ASDs.

## Conclusion

The physical aging behavior of HPMCAS was investigated using calorimetric techniques to probe its enthalpy recovery. HPMCAS exhibited a distinct enthalpy recovery at temperatures well below $T_g$ upon aging at $T_a$ < 353K. This was evident in the thermogram plots as a low temperature endotherm that resolved below $T_g$. $T_f$ calculations from these thermograms showed partial approach toward equilibrium to a plateau even at temperatures near $T_g$ and at $t_a$ up to 600 min. From these $T_f$ time evolutions, the physical aging rate was calculated and the results indicated a significant but small difference in the aging rate between HPMCAS aged near $T_g$ and that of HPMCAS aged well-below $T_g$. To further probe the source of this behavior, FTIR results were performed and they revealed chemical changes occurring over the course of aging. We hypothesize that these chemical changes contributed to the HPMCAS enthalpy recovery behavior. Upon aging, the functions of HPMCAS as an ASD excipient are expected to change, where thermal processing dictates the potential for molecular mobility well-below $T_g$ and in turn, phase separation in the ASD. This study warrants future investigations into how exactly HPMCAS exhibits the observed structural recovery behavior and the full extent of its effects on ASD drug stability and performance.

## Supporting Information

Additional $T_g$, TGA, and re-heating thermogram data regarding all three grades of HPMCAS (-LF, -MF, and -HF) and PS 16k. Schematic depicting the Moynihan method of fictive temperature calculation. A table for fitting parameters used for calculating aging rate. FTIR data of HPMCAS-LF aged at $T_a$ = 353K. Additional FTIR data of succinic acid, aged HPMCAS-LF, and untreated HPMCAS-LF.

## Acknowledgments

This work was supported by the National Science Foundation (NSF) Materials Research Science and Engineering Center Program through the Princeton Center for Complex Materials (PCCM) (DMR-2011750). The authors also thank Lonza Pharma (Bend,

Oregon) for donating the three grades of HPMCAS used for this study. The authors acknowledge the use of Princeton's Imaging and Analysis Center, which is partially supported through the Princeton Center for Complex Materials (PCCM), a National Science Foundation (NSF)-MRSEC program (DMR-2011750).

## References


(1) Amidon, G. L.; Lennernäs, H.; Shah, V. P.; Crison, J. R. A Theoretical Basis for a Biopharmaceutic Drug Classification: The Correlation of in Vitro Drug Product Dissolution and in Vivo Bioavailability. *Pharmaceutical Research: An Official Journal of the American Association of Pharmaceutical Scientists*. 1995, pp 413–420. https://doi.org/10.1023/A:1016212804288.

(2) Benet, L. Z. The Role of BCS (Biopharmaceutics Classification System) and BDDCS (Biopharmaceutics Drug Disposition Classification System) in Drug Development. *J. Pharm. Sci.* **2013**, *102* (1), 34–42. https://doi.org/https://doi.org/10.1002/jps.23359.

(3) Farrell, B.; French Merkley, V.; Ingar, N. Reducing Pill Burden and Helping with Medication Awareness to Improve Adherence. *Can. Pharm. J.* **2013**, *146* (5), 262–269. https://doi.org/10.1177/1715163513500208.

(4) Rigby, D. Value of Medication Reviews: Reducing Pill Burden. *AJP Aust. J. Pharm.* **2022**. https://doi.org/10.3316/informit.277606971212240.

(5) Chen, H.; Khemtong, C.; Yang, X.; Chang, X.; Gao, J. Nanonization Strategies for Poorly Water-Soluble Drugs. *Drug Discov. Today* **2011**, *16* (7–8), 354–360. https://doi.org/10.1016/j.drudis.2010.02.009.

(6) Stella, V. J.; Rao, V. M.; Zannou, E. A.; Zia, V. Mechanisms of Drug Release from Cyclodextrin Complexes. *Adv. Drug Deliv. Rev.* **1999**, *36* (1), 3–16. https://doi.org/10.1016/S0169-409X(98)00052-0.

(7) Pouton, C. W.; Porter, C. J. H. Formulation of Lipid-Based Delivery Systems for Oral Administration: Materials, Methods and Strategies. *Advanced Drug Delivery Reviews*. 2008. https://doi.org/10.1016/j.addr.2007.10.010.

(8) Avdeef, A. Solubility of Sparingly-Soluble Ionizable Drugs. *Advanced Drug Delivery Reviews*. 2007. https://doi.org/10.1016/j.addr.2007.05.008.

(9) Chan, O. H.; Schmid, H. L.; Stilgenbauer, L. A.; Howson, W.; Horwell, D. C.; Stewart, B. H. Evaluation of a Targeted Prodrug Strategy to Enhance Oral Absorption of Poorly Water-Soluble Compounds. *Pharm. Res.* **1998**. https://doi.org/10.1023/A:1011969808907.

(10) Schönfeld, B.; Westedt, U.; Wagner, K. G. Vacuum Drum Drying – A Novel Solvent-Evaporation Based Technology to Manufacture Amorphous Solid Dispersions in Comparison to Spray Drying and Hot Melt Extrusion. *Int. J. Pharm.* **2021**, *596* (January). https://doi.org/10.1016/j.ijpharm.2021.120233.

(11) Guo, Z.; Boyce, C.; Rhodes, T.; Liu, L.; Salituro, G. M.; Lee, K. joong; Bak, A.; Leung, D. H. A Novel Method for Preparing Stabilized Amorphous Solid Dispersion Drug Formulations Using Acoustic Fusion. *Int. J. Pharm.* **2021**, *592* (October), 120026. https://doi.org/10.1016/j.ijpharm.2020.120026.

(12) Ting, J. M.; Porter, W. W.; Mecca, J. M.; Bates, F. S.; Reineke, T. M. Advances in

Polymer Design for Enhancing Oral Drug Solubility and Delivery. *Bioconjugate Chemistry*. 2018. https://doi.org/10.1021/acs.bioconjchem.7b00646.

(13) Yu, L. Amorphous Pharmaceutical Solids: Preparation, Characterization and Stabilization. *Adv. Drug Deliv. Rev.* **2001**. https://doi.org/10.1016/S0169-409X(01)00098-9.

(14) Jermain, S. V.; Brough, C.; Williams, R. O. Amorphous Solid Dispersions and Nanocrystal Technologies for Poorly Water-Soluble Drug Delivery – An Update. *Int. J. Pharm.* **2018**. https://doi.org/10.1016/j.ijpharm.2017.10.051.

(15) Van Den Mooter, G. The Use of Amorphous Solid Dispersions: A Formulation Strategy to Overcome Poor Solubility and Dissolution Rate. *Drug Discov. Today Technol.* **2012**, *9* (2), e79–e85. https://doi.org/10.1016/j.ddtec.2011.10.002.

(16) Hancock, B. C.; Parks, M. What Is the True Solubility Advantage for Amorphous Pharmaceuticals? *Pharm. Res.* **2000**, *17* (4), 397–404. https://doi.org/10.1023/A:1007516718048.

(17) Murdande, S. B.; Pikal, M. J.; Shanker, R. M.; Bogner, R. H. Solubility Advantage of Amorphous Pharmaceuticals, Part 3: Is Maximum Solubility Advantage Experimentally Attainable and Sustainable? *J. Pharm. Sci.* **2011**, *100* (10), 4349–4356. https://doi.org/https://doi.org/10.1002/jps.22643.

(18) Paus, R.; Ji, Y.; Vahle, L.; Sadowski, G. Predicting the Solubility Advantage of Amorphous Pharmaceuticals: A Novel Thermodynamic Approach. *Mol. Pharm.* **2015**. https://doi.org/10.1021/mp500824d.

(19) Hancock, B. C.; Zografi, G. Characteristics and Significance of the Amorphous State in Pharmaceutical Systems. *J. Pharm. Sci.* **2002**, *86* (1), 1–12. https://doi.org/10.1021/js9601896.

(20) Donth, E.-J. Introduction. In *The Glass Transition: Relaxation Dynamics in Liquids and Disordered Materials*; Springer Berlin Heidelberg: Berlin, Heidelberg, 2001; pp 1–10. https://doi.org/10.1007/978-3-662-04365-3_1.

(21) RIEBLING, E. F. Structural Similarities Between a Glass and Its Melt. *J. Am. Ceram. Soc.* **1968**, *51* (3), 143–149. https://doi.org/https://doi.org/10.1111/j.1151-2916.1968.tb11857.x.

(22) Cowie, J. M. G.; Arrighi, V. Physical Aging of Polymer Blends. *Polym. Blends Handb.* **2014**, *20* (94), 1357–1394. https://doi.org/10.1007/978-94-007-6064-6_15.

(23) Huang, Y.; Wang, X.; Paul, D. R. Physical Aging of Thin Glassy Polymer Films: Free Volume Interpretation. *J. Memb. Sci.* **2006**. https://doi.org/10.1016/j.memsci.2005.10.032.

(24) Tool, A. Q. EFFECT OF HEAT-TREATMENT ON THE DENSITY AND CONSTITUTION OF HIGH-SILICA GLASSES OF THE BOROSILICATE TYPE. *J. Am. Ceram. Soc.* **1948**. https://doi.org/10.1111/j.1151-2916.1948.tb14287.x.

(25) Guo, Y.; Zhang, C.; Lai, C.; Priestley, R. D.; D'Acunzi, M.; Fytas, G. Structural

Relaxation of Polymer Nanospheres under Soft and Hard Confinement: Isobaric versus Isochoric Conditions. In *ACS Nano*; 2011. https://doi.org/10.1021/nn201751m.

(26) Koh, Y. P.; Simon, S. L. The Glass Transition and Enthalpy Recovery of a Single Polystyrene Ultrathin Film Using Flash DSC. *J. Chem. Phys.* **2017**, *146* (20). https://doi.org/10.1063/1.4979126.

(27) Sinko, C. M.; Yee, A. F.; Amidon, G. L. The Effect of Physical Aging on the Dissolution Rate of Anionic Polyelectrolytes. *Pharmaceutical Research: An Official Journal of the American Association of Pharmaceutical Scientists*. 1990, pp 648–653. https://doi.org/10.1023/A:1015882631082.

(28) Landry, C. J. T.; Lum, K. K.; O'Reilly, J. M. Physical Aging of Blends of Cellulose Acetate Polymers with Dyes and Plasticizers. *Polymer (Guildf).* **2001**, *42* (13), 5781–5792. https://doi.org/10.1016/S0032-3861(01)00018-0.

(29) Huang, Y.; Paul, D. R. Physical Aging of Thin Glassy Polymer Films Monitored by Gas Permeability. *Polymer (Guildf).* **2004**, *45* (25), 8377–8393. https://doi.org/10.1016/j.polymer.2004.10.019.

(30) Kucera, S. A.; Felton, L. A.; McGinity, J. W. Physical Aging in Pharmaceutical Polymers and the Effect on Solid Oral Dosage Form Stability. *Int. J. Pharm.* **2013**, *457* (2), 428–436. https://doi.org/https://doi.org/10.1016/j.ijpharm.2013.01.069.

(31) Aji, D. P. B.; Johari, G. P. Kinetic-Freezing and Unfreezing of Local-Region Fluctuations in a Glass Structure Observed by Heat Capacity Hysteresis. *J. Chem. Phys.* **2015**, *142* (21). https://doi.org/10.1063/1.4921782.

(32) Monnier, X.; Colmenero, J.; Wolf, M.; Cangialosi, D. Reaching the Ideal Glass in Polymer Spheres: Thermodynamics and Vibrational Density of States. *Phys. Rev. Lett.* **2021**, *126* (11), 118004. https://doi.org/10.1103/PhysRevLett.126.118004.

(33) Monnier, X.; Cangialosi, D. Thermodynamic Ultrastability of a Polymer Glass Confined at the Micrometer Length Scale. *Phys. Rev. Lett.* **2018**, *121* (13), 137801. https://doi.org/10.1103/PhysRevLett.121.137801.

(34) Perez-De Eulate, N. G.; Cangialosi, D. The Very Long-Term Physical Aging of Glassy Polymers. *Phys. Chem. Chem. Phys.* **2018**, *20* (18), 12356–12361. https://doi.org/10.1039/c8cp01940a.

(35) Monnier, X.; Marina, S.; de Pariza, X. L.; Sardón, H.; Martin, J.; Cangialosi, D. Physical Aging Behavior of a Glassy Polyether. *Polymers (Basel).* **2021**, *13* (6), 1–12. https://doi.org/10.3390/polym13060954.

(36) Androsch, R.; Jariyavidyanont, K.; Schick, C. Enthalpy Relaxation of Polyamide 11 of Different Morphology Far Below the Glass Transition Temperature. *Entropy* . 2019. https://doi.org/10.3390/e21100984.

(37) Righetti, M. C.; Mele, E. Structural Relaxation in PLLA: Contribution of Different Scale Motions. *Thermochim. Acta* **2019**, *672* (December 2018), 157–161. https://doi.org/https://doi.org/10.1016/j.tca.2018.12.027.

(38) Boucher, V. M.; Cangialosi, D.; Alegría, A.; Colmenero, J. Enthalpy Recovery of Glassy Polymers: Dramatic Deviations from the Extrapolated Liquidlike Behavior. *Macromolecules* **2011**, *44* (20), 8333–8342. https://doi.org/10.1021/ma2018233.

(39) Cangialosi, D.; Boucher, V. M.; Alegría, A.; Colmenero, J. Direct Evidence of Two Equilibration Mechanisms in Glassy Polymers. *Phys. Rev. Lett.* **2013**, *111* (9), 1–5. https://doi.org/10.1103/PhysRevLett.111.095701.

(40) Morvan, A.; Delpouve, N.; Vella, A.; Saiter-Fourcin, A. Physical Aging of Selenium Glass: Assessing the Double Mechanism of Equilibration and the Crystallization Process. *J. Non. Cryst. Solids* **2021**, *570*, 121013. https://doi.org/https://doi.org/10.1016/j.jnoncrysol.2021.121013.

(41) Hodge, I. M. Effects of Annealing and Prior History on Enthalpy Relaxation in Glassy Polymers. 4. Comparison of Five Polymers. *Macromolecules* **1983**, *16* (6), 898–902.

(42) Hodge, I. M.; Berens, A. R. Calculation of the Effects of Annealing on Sub-Tg Endotherms. *Macromolecules* **1981**, *14* (5), 1598–1599.

(43) Hodge, I. M. *Classical Relaxation Phenomenology*; Springer, 2019.

(44) Song, H.; Medvedev, G. A.; Caruthers, J. M. Structural Relaxation of an Epoxy Resin at Temperatures Well below Tg*. *Polym. Eng. \& Sci.* **2022**, *62* (2), 537–552. https://doi.org/https://doi.org/10.1002/pen.25866.

(45) Zhao, Y.; Inbar, P.; Chokshi, H. P.; Malick, A. W.; Choi, D. S. Prediction of the Thermal Phase Diagram of Amorphous Solid Dispersions by Flory–Huggins Theory. *J. Pharm. Sci.* **2011**, *100* (8), 3196–3207. https://doi.org/https://doi.org/10.1002/jps.22541.

(46) LaFountaine, J. S.; McGinity, J. W.; Williams, R. O. Challenges and Strategies in Thermal Processing of Amorphous Solid Dispersions: A Review. *AAPS PharmSciTech* **2016**. https://doi.org/10.1208/s12249-015-0393-y.

(47) Baird, J. A.; Taylor, L. S. Evaluation of Amorphous Solid Dispersion Properties Using Thermal Analysis Techniques. *Adv. Drug Deliv. Rev.* **2012**, *64* (5), 396–421. https://doi.org/10.1016/j.addr.2011.07.009.

(48) Purohit, H. S.; Taylor, L. S. Phase Separation Kinetics in Amorphous Solid Dispersions upon Exposure to Water. *Mol. Pharm.* **2015**, *12* (5), 1623–1635. https://doi.org/10.1021/acs.molpharmaceut.5b00041.

(49) Chen, H.; Pui, Y.; Liu, C.; Chen, Z.; Su, C. C.; Hageman, M.; Hussain, M.; Haskell, R.; Stefanski, K.; Foster, K.; et al. Moisture-Induced Amorphous Phase Separation of Amorphous Solid Dispersions: Molecular Mechanism, Microstructure, and Its Impact on Dissolution Performance. *J. Pharm. Sci.* **2018**. https://doi.org/10.1016/j.xphs.2017.10.028.

(50) Ishizuka, Y.; Ueda, K.; Okada, H.; Takeda, J.; Karashima, M.; Yazawa, K.; Higashi, K.; Kawakami, K.; Ikeda, Y.; Moribe, K. Effect of Drug–Polymer Interactions through Hypromellose Acetate Succinate Substituents on the

Physical Stability on Solid Dispersions Studied by Fourier-Transform Infrared and Solid-State Nuclear Magnetic Resonance. *Mol. Pharm.* **2019**, *16*, 2785–2794. https://doi.org/10.1021/acs.molpharmaceut.9b00301.

(51) Qi, S.; Moffat, J. G.; Yang, Z. Early Stage Phase Separation in Pharmaceutical Solid Dispersion Thin Films under High Humidity: Improved Spatial Understanding Using Probe-Based Thermal and Spectroscopic Nanocharacterization Methods. *Mol. Pharm.* **2013**, *10* (3), 918–930. https://doi.org/10.1021/mp300557q.

(52) Rumondor, A. C. F.; Marsac, P. J.; Stanford, L. A.; Taylor, L. S. Phase Behavior of Poly(Vinylpyrrolidone) Containing Amorphous Solid Dispersions in the Presence of Moisture. *Mol. Pharm.* **2009**, *6* (5), 1492–1505. https://doi.org/10.1021/mp900050c.

(53) Rumondor, A. C. F. F.; Wikström, H.; Van Eerdenbrugh, B.; Taylor, L. S. Understanding the Tendency of Amorphous Solid Dispersions to Undergo Amorphous-Amorphous Phase Separation in the Presence of Absorbed Moisture. *AAPS PharmSciTech* **2011**, *12* (4), 1209–1219. https://doi.org/10.1208/s12249-011-9686-y.

(54) Karmwar, P.; Graeser, K.; Gordon, K. C.; Strachan, C. J.; Rades, T. Investigation of Properties and Recrystallisation Behaviour of Amorphous Indomethacin Samples Prepared by Different Methods. *Int. J. Pharm.* **2011**, *417* (1–2), 94–100. https://doi.org/10.1016/j.ijpharm.2010.12.019.

(55) Mugheirbi, N. A.; Marsac, P. J.; Taylor, L. S. Insights into Water-Induced Phase Separation in Itraconazole-Hydroxypropylmethyl Cellulose Spin Coated and Spray Dried Dispersions. *Mol. Pharm.* **2017**, *14* (12), 4387–4402. https://doi.org/10.1021/acs.molpharmaceut.7b00499.

(56) Bhattacharya, S.; Suryanarayanan, R. Local Mobility in Amorphous Pharmaceuticals—Characterization and Implications on Stability. *J. Pharm. Sci.* **2009**, *98* (9), 2935–2953. https://doi.org/https://doi.org/10.1002/jps.21728.

(57) Bhardwaj, S. P.; Arora, K. K.; Kwong, E.; Templeton, A.; Clas, S. D.; Suryanarayanan, R. Mechanism of Amorphous Itraconazole Stabilization in Polymer Solid Dispersions: Role of Molecular Mobility. *Mol. Pharm.* **2014**, *11* (11), 4228–4237. https://doi.org/10.1021/mp5004515.

(58) Kothari, K.; Ragoonanan, V.; Suryanarayanan, R. The Role of Polymer Concentration on the Molecular Mobility and Physical Stability of Nifedipine Solid Dispersions. *Mol. Pharm.* **2015**, *12* (5), 1477–1484. https://doi.org/10.1021/mp500800c.

(59) Mehta, M.; Kothari, K.; Ragoonanan, V.; Suryanarayanan, R. Effect of Water on Molecular Mobility and Physical Stability of Amorphous Pharmaceuticals. *Mol. Pharm.* **2016**, *13* (4), 1339–1346. https://doi.org/10.1021/acs.molpharmaceut.5b00950.

(60) Ricarte, R. G.; Van Zee, N. J.; Li, Z.; Johnson, L. M.; Lodge, T. P.; Hillmyer, M. A. Recent Advances in Understanding the Micro- and Nanoscale Phenomena of

Amorphous Solid Dispersions. *Mol. Pharm.* **2019**. https://doi.org/10.1021/acs.molpharmaceut.9b00601.

(61) Owusu-Ware, S. K.; Boateng, J. S.; Chowdhry, B. Z.; Antonijevic, M. D. Glassy State Molecular Mobility and Its Relationship to the Physico-Mechanical Properties of Plasticized Hydroxypropyl Methylcellulose (HPMC) Films. *Int. J. Pharm. X* **2019**, *1* (June), 100033. https://doi.org/10.1016/j.ijpx.2019.100033.

(62) Kawakami, K.; Ida, Y. Direct Observation of the Enthalpy Relaxation and the Recovery Processes of Maltose-Based Amorphous Formulation by Isothermal Microcalorimetry. *Pharm. Res.* **2003**, *20* (9), 1430–1436.

(63) Dalsania, S.; Sharma, J.; Munjal, B.; Bansal, A. K. Impact of Drug-Polymer Miscibility on Enthalpy Relaxation of Irbesartan Amorphous Solid Dispersions. *Pharm. Res.* **2018**, *35* (2). https://doi.org/10.1007/s11095-017-2296-y.

(64) Bansal, S. S.; Kaushal, A. M.; Bansal, A. K. Enthalpy Relaxation Studies of Two Structurally Related Amorphous Drugs and Their Binary Dispersions. *Drug Dev. Ind. Pharm.* **2010**, *36* (11), 1271–1280. https://doi.org/10.3109/03639041003753847.

(65) Lapuk, S. E.; Ponomareva, M. A.; Galukhin, A. V.; Mukhametzyanov, T. A.; Schick, C.; Gerasimov, A. V. Glass Transition Kinetics and Physical Aging of Polyvinylpyrrolidones with Different Molecular Masses. *Macromolecules* **2022**. https://doi.org/10.1021/acs.macromol.2c00547.

(66) Friesen, D. T.; Shanker, R.; Crew, M.; Smithey, D. T.; Curatolo, W. J.; Nightingale, J. A. S. Hydroxypropyl Methylcellulose Acetate Succinate-Based Spray-Dried Dispersions: An Overview. *Mol. Pharm.* **2008**. https://doi.org/10.1021/mp8000793.

(67) Ting, J. M.; Navale, T. S.; Jones, S. D.; Bates, F. S.; Reineke, T. M. Deconstructing HPMCAS: Excipient Design to Tailor Polymer-Drug Interactions for Oral Drug Delivery. *ACS Biomater. Sci. Eng.* **2015**, *1* (10), 978–990. https://doi.org/10.1021/acsbiomaterials.5b00234.

(68) Newman, A.; Knipp, G.; Zografi, G. Assessing the Performance of Amorphous Solid Dispersions. *Journal of Pharmaceutical Sciences*. 2012. https://doi.org/10.1002/jps.23031.

(69) Abate, A. A.; Cangialosi, D.; Napolitano, S. High Throughput Optimization Procedure to Characterize Vitrification Kinetics. *Thermochim. Acta* **2022**, *707* (November 2021), 179084. https://doi.org/10.1016/j.tca.2021.179084.

(70) MOYNIHAN, C. T.; EASTEAL, A. J.; De BOLT, M. A.; TUCKER, J. Dependence of the Fictive Temperature of Glass on Cooling Rate. *J. Am. Ceram. Soc.* **1976**. https://doi.org/10.1111/j.1151-2916.1976.tb09376.x.

(71) Moynihan, C. T.; Macedo, P. B.; Montrose, C. J.; Montrose, C. J.; Gupta, P. K.; DeBolt, M. A.; Dill, J. F.; Dom, B. E.; Drake, P. W.; Easteal, A. J.; et al. STRUCTURAL RELAXATION IN VITREOUS MATERIALS. *Ann. N. Y. Acad. Sci.*

**1976**. https://doi.org/10.1111/j.1749-6632.1976.tb39688.x.

(72) Hodge, I. M.; Berens, A. R. Effects of Annealing and Prior History on Enthalpy Relaxation in Glassy Polymers. 2. Mathematical Modeling. *Macromolecules* **1982**, *15* (3), 762–770.

(73) Gao, M.; Perepezko, J. H. Separating $\ensuremath{\beta}$ Relaxation from $\ensuremath{\alpha}$ Relaxation in Fragile Metallic Glasses Based on Ultrafast Flash Differential Scanning Calorimetry. *Phys. Rev. Mater.* **2020**, *4* (2), 25602. https://doi.org/10.1103/PhysRevMaterials.4.025602.

(74) Yang, Q.; Peng, S. X.; Wang, Z.; Yu, H. Bin. Shadow Glass Transition as a Thermodynamic Signature of β Relaxation in Hyper-Quenched Metallic Glasses. *Natl. Sci. Rev.* **2020**, *7* (12), 1896–1905. https://doi.org/10.1093/nsr/nwaa100.

(75) Fan, J.; Cooper, E. I.; Angell, C. A. Glasses with Strong Calorimetric β-Glass Transitions and the Relation to the Protein Glass Transition Problem. *J. Phys. Chem.* **1994**, *98* (37), 9345–9349. https://doi.org/10.1021/j100088a041.

(76) Peng, S.; Cheng, Y.; Pries, J.; Wei, S.; Yu, H.; Wuttig, M. Uncovering □ - Relaxations in Amorphous Phase-Change Materials. **2020**, No. January, 1–9.

(77) Tombari, E.; Johari, G. P. Endothermic Effects on Heating Physically Aged Sucrose Glasses and the Clausius Theorem Violation in Glass Thermodynamics. *J. Phys. Chem. B* **2020**, *124* (10), 2017–2028. https://doi.org/10.1021/acs.jpcb.9b10937.

(78) Hodge, I. M.; Berens, A. R. Effects of Annealing and Prior History on Enthalpy Relaxation in Glassy Polymers. 5. Mathematical Modeling of Nonthermal Preaging Perturbations. *Macromolecules* **1985**, *18* (10), 1980–1984. https://doi.org/10.1021/ma00152a030.

(79) Robertson, C. G.; Monat, J. E.; Wilkes, G. L. Physical Aging of an Amorphous Polyimide: Enthalpy Relaxation and Mechanical Property Changes. *J. Polym. Sci. Part B Polym. Phys.* **1999**, *37* (15), 1931–1946. https://doi.org/10.1002/(SICI)1099-0488(19990801)37:15<1931::AID-POLB17>3.0.CO;2-I.

(80) Zhao, J.; Simon, S. L.; McKenna, G. B. Using 20-Million-Year-Old Amber to Test the Super-Arrhenius Behaviour of Glass-Forming Systems. *Nat. Commun.* **2013**, *4*, 1–6. https://doi.org/10.1038/ncomms2809.

(81) Cangialosi, D. Dynamics and Thermodynamics of Polymer Glasses. *J. Phys. Condens. Matter* **2014**, *26* (15). https://doi.org/10.1088/0953-8984/26/15/153101.

(82) Frieberg, B.; Glynos, E.; Green, P. F. Structural Relaxations of Thin Polymer Films. *Phys. Rev. Lett.* **2012**, *108* (26), 268304. https://doi.org/10.1103/PhysRevLett.108.268304.

(83) Frieberg, B. R.; Glynos, E.; Sakellariou, G.; Tyagi, M.; Green, P. F. Effect of Molecular Stiffness on the Physical Aging of Polymers. *Macromolecules* **2020**, *53* (18), 7684–7690. https://doi.org/10.1021/acs.macromol.0c01331.

(84) Pye, J. E.; Rohald, K. A.; Baker, E. A.; Roth, C. B. Physical Aging in Ultrathin Polystyrene Films: Evidence of a Gradient in Dynamics at the Free Surface and Its Connection to the Glass Transition Temperature Reductions. *Macromolecules* **2010**, *43* (19), 8296–8303. https://doi.org/10.1021/ma101412r.

(85) Priestley, R. D.; Broadbelt, L. J.; Torkelson, J. M. Physical Aging of Ultrathin Polymer Films above and below the Bulk Glass Transition Temperature: Effects of Attractive vs Neutral Polymer−Substrate Interactions Measured by Fluorescence. *Macromolecules* **2005**, *38* (3), 654–657. https://doi.org/10.1021/ma047994o.

(86) Ngai, K. L. The Origin of the Faster Mechanism of Partial Enthalpy Recovery Deep in the Glassy State of Polymers. *Phys. Chem. Chem. Phys.* **2021**, *23* (24), 13468–13472. https://doi.org/10.1039/d1cp01445e.

(87) Ngai, K. L.; Capaccioli, S.; Wang, L.-M. Segmental α-Relaxation for the First Step and Sub-Rouse Modes for the Second Step in Enthalpy Recovery in the Glassy State of Polystyrene. *Macromolecules* **2019**, *52* (4), 1440–1446. https://doi.org/10.1021/acs.macromol.8b02125.

(88) Wisitsorasak, A.; Wolynes, P. G. Dynamical Heterogeneity of the Glassy State. *J. Phys. Chem. B* **2014**, *118* (28), 7835–7847. https://doi.org/10.1021/jp4125777.

(89) Song, Z.; Rodríguez-Tinoco, C.; Mathew, A.; Napolitano, S. Fast Equilibration Mechanisms in Disordered Materials Mediated by Slow Liquid Dynamics. *Sci. Adv.* **2022**, *8* (15), eabm7154. https://doi.org/10.1126/sciadv.abm7154.

(90) Koh, Y. P.; Simon, S. L. Enthalpy Recovery of Polystyrene: Does a Long-Term Aging Plateau Exist? *Macromolecules* **2013**, *46* (14), 5815–5821. https://doi.org/10.1021/ma4011236.

(91) Song, L.; Xu, W.; Huo, J.; Wang, J. Q.; Wang, X.; Li, R. Two-Step Relaxations in Metallic Glasses during Isothermal Annealing. *Intermetallics* **2018**, *93* (October 2017), 101–105. https://doi.org/10.1016/j.intermet.2017.11.016.

(92) Liu, C. F.; Zhang, A. P.; Li, W. Y.; Yue, F. X.; Sun, R. C. Succinoylation of Cellulose Catalyzed with Iodine in Ionic Liquid. *Ind. Crops Prod.* **2010**, *31* (2), 363–369. https://doi.org/10.1016/j.indcrop.2009.12.002.

(93) Li, J.; Zhang, L. P.; Peng, F.; Bian, J.; Yuan, T. Q.; Xu, F.; Sun, R. C. Microwave-Assisted Solvent-Free Acetylation of Cellulose with Acetic Anhydride in the Presence of Iodine as a Catalyst. *Molecules* **2009**, *14* (9), 3551–3566. https://doi.org/10.3390/molecules14093551.

(94) Hu, W.; Chen, S.; Xu, Q.; Wang, H. Solvent-Free Acetylation of Bacterial Cellulose under Moderate Conditions. *Carbohydr. Polym.* **2011**, *83* (4), 1575–1581. https://doi.org/10.1016/j.carbpol.2010.10.016.

(95) Ashori, A.; Babaee, M.; Jonoobi, M.; Hamzeh, Y. Solvent-Free Acetylation of Cellulose Nanofibers for Improving Compatibility and Dispersion. *Carbohydr. Polym.* **2014**, *102* (1), 369–375. https://doi.org/10.1016/j.carbpol.2013.11.067.

(96) Lin, N.; Huang, J.; Chang, P. R.; Feng, J.; Yu, J. Surface Acetylation of Cellulose Nanocrystal and Its Reinforcing Function in Poly(Lactic Acid). *Carbohydr. Polym.* **2011**, *83* (4), 1834–1842. https://doi.org/10.1016/j.carbpol.2010.10.047.

(97) Jebrane, M.; Harper, D.; Labbé, N.; Sbe, G. Comparative Determination of the Grafting Distribution and Viscoelastic Properties of Wood Blocks Acetylated by Vinyl Acetate or Acetic Anhydride. *Carbohydr. Polym.* **2011**, *84* (4), 1314–1320. https://doi.org/10.1016/j.carbpol.2011.01.026.